

TOWARD A LONG-LIFETIME POLARIZED PHOTOELECTRON GUN FOR THE Ce^+BAF POSITRON SOURCE*

M. W. Bruker[†], J. Grames, C. Hernández-García, A. Hofler, G. Palacios-Serrano,
Thomas Jefferson National Accelerator Facility, Newport News, VA, USA

Abstract

The addition of spin-polarized, continuous-wave (c.w.) positron beams to the 12 GeV Continuous Electron Beam Accelerator Facility (CEBAF) would provide a significant capability to the experimental nuclear physics program at Jefferson Lab. Based on bremsstrahlung and pair-production in a high-Z target, the positron source requires a 120 MeV spin-polarized c.w. electron beam of several milliamperes. While the beam dynamics of the high-current electron beam are tenable, sustaining this current for weeks of user operations requires an unprecedented charge lifetime from a high-polarization GaAs-based photocathode. A promising approach to exceed the kilocoulomb charge lifetime barrier is reducing the ion back-bombardment fluence at the photocathode. By increasing the laser size and managing the emittance growth with an adequate cathode/anode design, significantly enhanced charge lifetime may be achieved. Based upon a new simulation model that qualitatively explains the lifetime data previously measured at different spot sizes, we describe the practical implications on the parameter space available for a kilocoulomb-lifetime polarized photogun design.

INTRODUCTION

Jefferson Lab aims to develop a capability to generate a spin-polarized, c.w. positron beam for injection into the main CEBAF accelerator and subsequent delivery to the experimental halls [1, 2]. The PEPPo method [3] will be used to generate positrons in a target subjected to a spin-polarized electron beam of at least 1 mA, the high current being necessary due to the low yield of the conversion and subsequent capture process. An overview of the envisioned facility (referred to as Ce^+BAF) and its electron injector can be found in [4, 5].

Generating a highly spin-polarized electron beam generally involves a DC-biased photogun with a GaAs photocathode activated with negative electron affinity (NEA) [6]. When illuminated with laser light of a certain wavelength, the surface of such a cathode emits an electron current proportional to the laser power; the average number of electrons per incident photon is referred to as the *quantum efficiency* (QE), η . Governed by the local chemical surface composition, the QE can be a function of transverse position as well as time. It is degraded by a variety of damage mechanisms, many of which have been identified and reduced to negligible levels over the years [7, 8]. The dominant remaining effect is *ion back-bombardment*, i.e., electron-impact ioniza-

tion of residual gas molecules and subsequent acceleration of the ions toward the cathode, where they degrade the QE through sputtering and implantation [9, 10]. The number of ions generated is proportional to the extracted charge Q , giving rise to an exponential decay with a *charge lifetime* τ according to

$$\eta(Q) \propto \exp(-Q/\tau). \quad (1)$$

While this decay is observed for a given laser-spot position on the photocathode, the QE is a local property; its local degradation depends on the position and energy distribution of the incident ions, which in turn is governed by the shape and trajectory of the electron beam causing the ionization as well as the geometry of the electrostatic field experienced by the ions. Assuming the sensitivity of the photocathode to ion damage cannot be changed, any improvement in lifetime has to involve altering the distribution and number of ions incident on the photocathode. Applying a positive voltage to the anode has been shown to eliminate the deleterious effects of ions generated downstream by electrostatically repelling them [11]. With the remaining ions being generated inside the accelerating gap, further improvements may be gained by lowering the density of gas molecules in the gap, i.e., the vacuum pressure, but order-of-magnitude improvements in this area would require a technological breakthrough.

The next best strategy is to accept a certain number of ions will hit the cathode, but to distribute their damage, ideally to an area where the QE is unimportant. For this reason, photoguns are routinely operated with the laser spot placed away from the electrostatic center to prevent ions generated far away from the cathode, which tend to get displaced by the electrostatic field, from damaging the area being illuminated [12]. However, the ionization cross section being largest at low electron energies ≤ 100 eV for all relevant gas species [13] results in a large number of ions being generated close to the cathode and, therefore, hitting the cathode with the same transverse distribution as that of the electron beam. Experiments at CEBAF have shown that an increase in lifetime can be attained by increasing the laser-spot size, thereby spreading out the damage over a larger area [14]. The simulations described here explore the scalability and limits of this approach.

ION SIMULATIONS

Although the dependency of the QE damage on the kinetic energy of the incident ions is not precisely known, the particle dynamics of the problem lend themselves well to numerical simulation, allowing us to compute the ion distribution on the photocathode for a given laser profile and QE distribution. Using the tracking code GPT [15], we

* Work supported by the U.S. Department of Energy, Office of Science, Office of Nuclear Physics under contract DE-AC05-06OR23177.

[†] bruker@jlab.org

track a particle ensemble representing the electron beam through the gun field (using the T-shape gun [16] with the cathode at -130 kV and the anode at $+2$ kV as an instructive example). The electrons are generated by randomly sampling the laser profile weighted with the QE distribution, which are stored on a 1000×1000 grid, enforcing a certain number of particles and total charge to represent a constant extracted current. The IONATOR element [13] then creates ions along the trajectory, which are also tracked through the field and measured by a screen coincident with the cathode surface. The incremental evolution of the QE distribution as a function of charge is obtained by repeating this process in a loop [17], modifying the QE for each grid tile according to a *damage function* F in each step:

$$\eta_{\text{new}} = \eta_{\text{old}} F := \eta_{\text{old}} \exp(-\alpha E_{\text{kin}}) \quad (2)$$

with E_{kin} being the total kinetic energy of the ions deposited in that grid tile. Figure 1 illustrates the idea. The damage function is a simple model for the physics of ion damage, allowing us to get qualitative results; the value of α determines the granularity of discretization. While the number of ions is proportional to both bunch charge and gas density, the former affects the dynamics due to space charge; we therefore overestimate the gas density by many orders of magnitude to get a meaningful number of ions. We choose a total gas density of $3 \times 10^{21} \text{ m}^{-3}$, corresponding to 0.1 mbar, to create about 80 000 ions per time step. The simulated gas composition is 90 % H_2 and 10 % CH_4 , representative of a typical baked gun chamber with ample non-evaporable getter pumping.

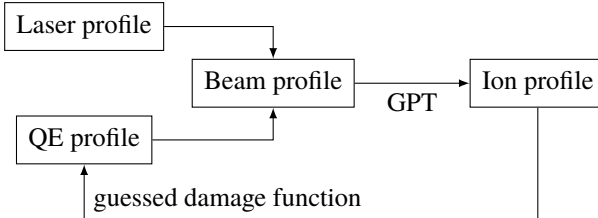


Figure 1: Principle of simulating QE degradation [17].

SCALING THE LASER-SPOT SIZE

While the QE lifetime may be naively expected to be proportional to the laser-spot area due to dilution of the resulting ion damage, experimental data suggest the actual scaling is less favorable, flattening out towards large spot sizes [14]. Figure 2 illustrates that two main effects conspire to cause this saturation:

1. The damage from high-energy ions (i.e., those generated far away from the photocathode) is displaced with respect to the laser spot, both because the electron beam generating them is focused away from the spot and because the ions are themselves subject to focusing and/or defocusing forces. Increasing the laser-spot size therefore results in sampling of more damaged area.

2. Any laser light outside of the active area does not contribute to the beam profile; as soon as the beam stops growing, so does the ion distribution.

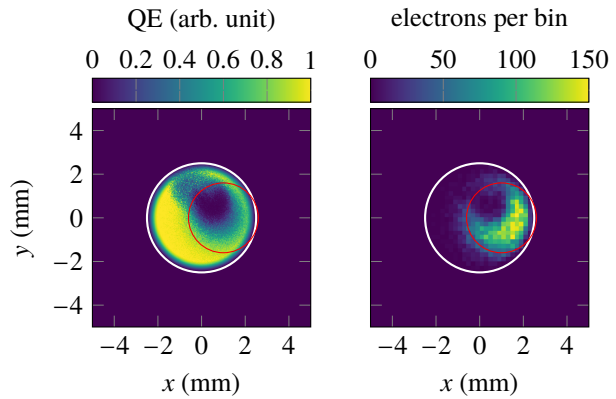


Figure 2: QE distribution (left) and electron distribution at emission (right) after 50 time steps with a Gaussian laser profile of $\sigma = 0.8$ mm. The red circle has a radius of 2σ , encompassing 86 % of the particles. The white circle represents the active area with a radius of 2.5 mm.

Figure 3 shows how the QE decays as a function of time (i.e., extracted charge); note that the decay is not strictly exponential because the beam profile changes over time, so the lifetime tends to be underestimated. While the integral of the laser profile (representing power) is kept constant, the initial QE not being the same in all cases is a result of the tails of the large laser spots lying outside the active area.

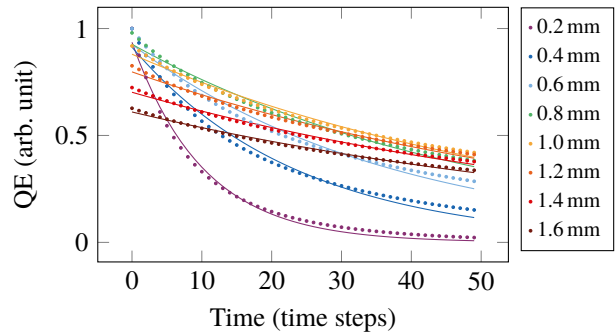


Figure 3: QE decay as a function of discrete time for the T-shape gun at -130 kV with different laser-spot sizes at $x = y = 0$, active area $r = 2.5$ mm. The legend corresponds to the σ of the Gaussian laser profile.

The so-obtained time constants are aggregated per spot size for different active-area radii in Fig. 4. The results indicate that an increase in spot size needs to be accompanied by a corresponding increase in spot displacement to prevent the emission area from sampling the damage from high-energy ions; also, the active area must be made large enough to accommodate the whole laser spot if a lifetime benefit is to be gained.

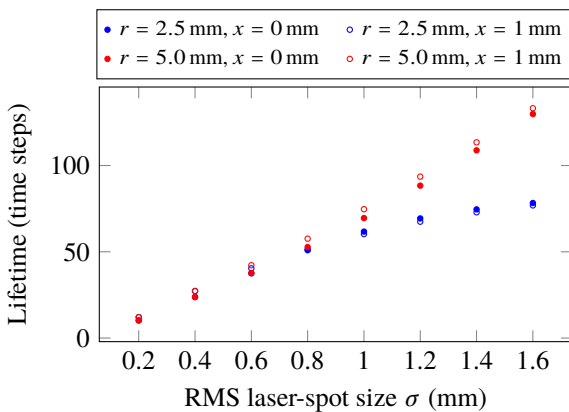


Figure 4: Lifetime as a function of laser-spot size for active areas of different radii r and different horizontal laser-spot displacements x .

ELECTROSTATIC OPTICS

In order to design a gun that supports a large laser spot while maximally suppressing ion damage coincident with the illuminated area, a trade-off with the beam parameters is necessary. While the thermal emittance inevitably scales with the spot radius, further contributions to it can come from space charge and aberrations of the gun field. It is possible to design electrodes providing a focusing and accelerating field without any spherical aberration [18], but the available focusing is limited and the physical size large. Before investing in such design work, we must first ascertain the focal properties needed.

To study the ion trajectories as a function of field geometry in isolation, it is instructive to remove any aberrations by simplifying the gun to a 1-d field, i.e., $E_z(z)$, giving $E_r(r, z) = -\frac{r}{2} \frac{\partial E_z}{\partial z}$ per Gauss's law in the case of cylindrical symmetry. Figure 5 shows how the ion distributions arriving at the cathode compare between two hypothetical fields, one with a focusing cathode, the other with a flat cathode.

It is apparent that the behavior can be divided into two ranges of z coordinates in which the ions originate. Low-to-medium-energy ions (those created at small z , i.e., close to the cathode) strike the cathode at the same transverse coordinate as their point of origin, which is in turn determined by the envelope of the electron beam. Ions generated close to the anode are additionally focused by the anode field, displacing them further away from the emission spot (note that focusing and defocusing fields are reversed for electrons vs. ions). The focusing gun quickly deflects the beam away from the laser spot, displacing most medium-energy ion damage to where it is inconsequential; the radial field at the cathode, which is defocusing for ions, has a comparatively small effect on their trajectories after they are generated. In contrast, the non-focusing gun places most ions coincident with the laser spot, diminishing the benefits of spot displacement. More generally, we conclude that apart from supporting a large laser spot, the field of a long-lifetime gun should be designed to deflect the beam away from the laser

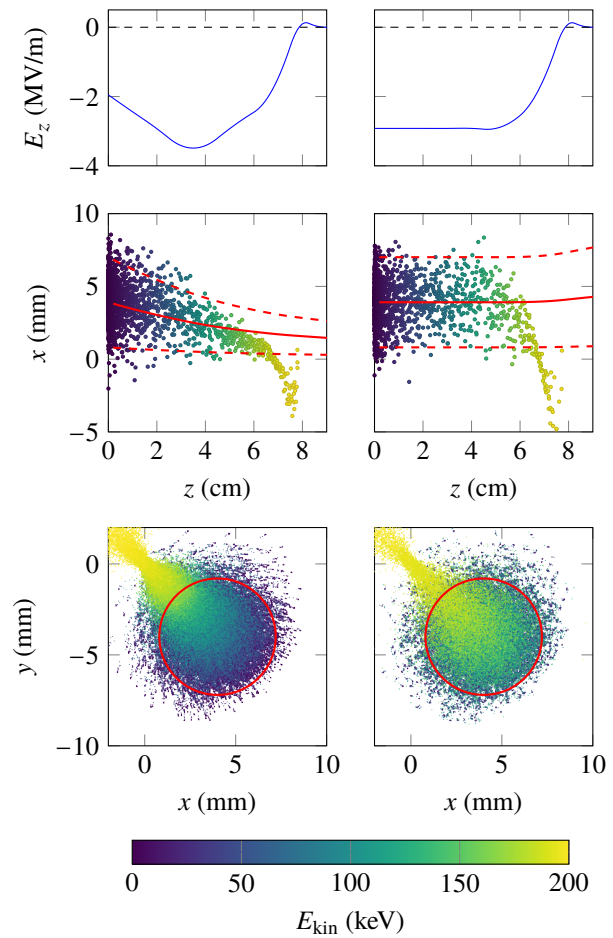


Figure 5: Electric field (top) and ion distribution on the photocathode (middle, bottom) for hypothetical focusing (left) and non-focusing (right) guns biased at -200 kV and having a potential barrier at the anode ($z = 8$ cm). The middle plot shows the x coordinate at which the ions hit the photocathode as a function of their longitudinal point of origin, whereas the bottom plot shows their 2-d transverse distribution on the photocathode plane. The laser spot is Gaussian with $\sigma = 1.6$ mm and is displaced by 4 mm in both x and y . The $\pm 2\sigma$ beam envelope is shown in red for comparison.

spot as close to the cathode as possible, likely by a combination of radial focusing and an extra dipole field, which our inverted-insulator guns parasitically include already [16].

THE PATH FORWARD

Our simulations of ion-bombardment-limited lifetime in photoguns open a path to a gun design able to attain a kilocoulomb-level charge lifetime from GaAs while providing beam parameters suitable for the Ce^+BAF driver. A realistic design will include an electrode geometry providing low-aberration focusing optics while able to operate at a cathode bias of at least -200 kV. In parallel, further experimental studies of existing guns are needed to validate the models for prediction of lifetime scaling.

REFERENCES

[1] J. Arrington *et al.*, “Physics with CEBAF at 12 GeV and future opportunities,” *Progress in Particle and Nuclear Physics*, vol. 127, p. 103 985, 2022.
doi:10.1016/j.ppnp.2022.103985

[2] A. Accardi *et al.*, “An experimental program with high duty-cycle polarized and unpolarized positron beams at Jefferson Lab,” *The European Physical Journal A*, vol. 57, no. 8, p. 261, 2021. doi:10.1140/epja/s10050-021-00564-y

[3] D. Abbott *et al.*, “Production of highly polarized positrons using polarized electrons at MeV energies,” *Phys. Rev. Lett.*, vol. 116, p. 214 801, 21 2016.
doi:10.1103/PhysRevLett.116.214801

[4] J. Grames *et al.*, “Positron beams at Ce+BAF,” in *Proc. IPAC’23*, Venice, Italy, 2023, pp. 896–899.
doi:10.18429/JACoW-IPAC2023-MOPC52

[5] R. Kazimi *et al.*, “Polarized electron injector for positron production at CEBAF,” in *Proc. IPAC’23*, Venice, Italy, 2023, pp. 2727–2730.
doi:10.18429/JACoW-IPAC2023-WEPA035

[6] T. Rao and D. H. Dowell, Eds., *An engineering guide to photoinjectors*. 2013. doi:10.48550/arXiv.1403.7539

[7] K. Aulenbacher *et al.*, “The MAMI source of polarized electrons,” *Nuclear Instruments and Methods in Physics Research Section A: Accelerators, Spectrometers, Detectors and Associated Equipment*, vol. 391, no. 3, pp. 498–506, 1997.
doi:10.1016/S0168-9002(97)00528-7

[8] C. K. Sinclair *et al.*, “Development of a high average current polarized electron source with long cathode operational lifetime,” *Phys. Rev. ST Accel. Beams*, vol. 10, p. 023 501, 2 2007. doi:10.1103/PhysRevSTAB.10.023501

[9] M. L. Stutzman and J. Grames, “Superlattice Photocathode Damage Analysis,” *AIP Conference Proceedings*, vol. 1149, no. 1, pp. 1032–1037, 2009. doi:10.1063/1.3215588

[10] V. Shutthanandan *et al.*, “Surface science analysis of GaAs photocathodes following sustained electron beam delivery,” *Phys. Rev. ST Accel. Beams*, vol. 15, p. 063 501, 6 2012.
doi:10.1103/PhysRevSTAB.15.063501

[11] J. Grames *et al.*, “A Biased Anode to Suppress Ion Back-Bombardment in a DC High Voltage Photoelectron Gun,” *AIP Conference Proceedings*, vol. 980, no. 1, pp. 110–117, 2008. doi:10.1063/1.2888075

[12] J. Grames *et al.*, “Charge and fluence lifetime measurements of a dc high voltage GaAs photogun at high average current,” *Phys. Rev. ST Accel. Beams*, vol. 14, p. 043 501, 4 2011.
doi:10.1103/PhysRevSTAB.14.043501

[13] J. Yoskowitz, J. Grames, G. Krafft, G. M. Soto, C. Valerio, and S. van der Geer, “Simulating Electron Impact Ionization Using a General Particle Tracer (GPT) Custom Element,” in *Proc. IPAC’21*, Campinas, SP, Brazil, 2021, paper WEPAB105, pp. 2843–2846.
doi:10.18429/JACoW-IPAC2021-WEPA105

[14] J. Grames *et al.*, “Milliampere Beam Studies using High Polarization Photocathodes at the CEBAF Photoinjector,” in *Proceedings of XVII International Workshop on Polarized Sources, Targets & Polarimetry — PoS(PSTP2017)*, vol. 324, 2018, p. 014. doi:10.22323/1.324.0014

[15] Pulsar Physics, *General Particle Tracer*. <http://www.pulsar.nl/gpt>

[16] P. A. Adderley *et al.*, “Load-locked dc high voltage GaAs photogun with an inverted-geometry ceramic insulator,” *Phys. Rev. ST Accel. Beams*, vol. 13, p. 010 101, 1 2010.
doi:10.1103/PhysRevSTAB.13.010101

[17] M. Bruker *et al.*, “New Results at JLab Describing Operating Lifetime of GaAs Photo-guns,” in *Proc. 5th Int. Particle Accel. Conf. (NAPAC’22)*, Albuquerque, NM, USA, 2022, paper WEPA13, pp. 644–647.
doi:10.18429/JACoW-NAPAC2022-WEPA13

[18] W. Peter and M. E. Jones, “Theory of high-brightness electron-beam production from photocathodes,” *Particle Accelerators*, vol. 24, pp. 231–243, 1989.